IEEE Access
Multidisciplinary ⋮ Rapid Review ⋮ Open Access Journal

Received November 27, 2018, accepted November 30, 2018, date of publication December 13, 2018, date of current version January 7, 2019.

Digital Object Identifier 10.1109/ACCESS.2018.2886424

Output Voltage Identification Based on Transmitting Side Information for Implantable Wireless Power Transfer System

XIANGTIAN MENG, DONGYUAN QIU, (Member, IEEE), MANHAO LIN, SAI CHUN TANG, AND BO ZHANG
School of Electric Power, South China University of Technology, Guangzhou 510641, China

Corresponding author: Dongyuan Qiu (epdyqiu@scut.edu.cn)

This work was supported in part by the National Natural Science Foundation of China under Grant 51677074 and in part by the Key Program of National Natural Science Foundation of China under Grant 51437005.

ABSTRACT Wireless power transfer (WPT) offers a promising solution to power implantable medical devices (IMDs). Due to the variations of mutual inductance and load, the output voltage of the implantable WPT system is easily unstable. To maintain a constant voltage for IMDs' operation, a novel method to identify the output voltage of the WPT system without any direct measurement on the receiving side is presented in this paper, where only the input voltage and current need to be measured. First, the output voltage identification of the WPT system is applied to the classic series–parallel compensation network. Next, an improved WPT system with S-LCL compensation network is proposed, which has the advantage that the output voltage identification is independent of mutual inductance and load resistance. Moreover, the characteristic analysis of the proposed WPT system is carried out, which proves its performance of high transfer efficiency. Finally, the WPT prototype with the S-LCL compensation network is built and tested. The experimental results are provided to further verify the correctness of theoretical analysis.

INDEX TERMS Wireless power transfer (WPT), output voltage identification, implantable medical device (IMD), compensation network.

I. INTRODUCTION

Implantable medical device (IMD) is an electronic device embedded in the human body, which are mainly used to monitor changes in physiological parameters [1], [2], diagnose and treat some diseases [3], [4] and replace dysfunctional organs [5]–[7]. Because of its prominent role, IMD has become an extremely important part of biomedical electronics, and has been more prevalent in medicinal applications. Electronic IMDs mainly include capsule endoscopy [8]–[10], cardiac pacemaker [11], [12], artificial heart [13], [14], spinal cord stimulator [15]–[19] and implanted sensor devices [20]. In general, most IMDs consists of external part and implantable part [21], the fundamental function of the system mainly focuses on the power supply and information exchange between external part and implantable part.

Initially, transcutaneous wire [22] was adopted through skin to power IMDs, but there is the risk of infections. At present, lithium battery is the most common power supply for IMDs [23]. Due to limited space for implants in human body, the size of the implanted battery is strictly controlled, which means that the capacity of implanted battery will not be large. When the battery runs out, surgery is needed to replace it, which increases physical and financial burden of patient. In contrast, magnetic resonance-based wireless power transfer (WPT) technique, which enables the electric power transferring from the transmitter to the receiver over an air gap, shows an enormous advantage of powering IMDs [24]–[26].

The typical WPT system for IMDs consists of the communication module and the energy transfer module, as shown in Fig.1. The communication module transmits the monitored data in vivo to the external part and sends the control instruction to the implanted part. The typical energy transfer module includes the DC power supply, the high-frequency (HF) inverter, the transmitting and receiving coils with compensation capacitors, the rectifier and the DC regulator [27]. The input DC voltage is inverted to an AC voltage by the HF

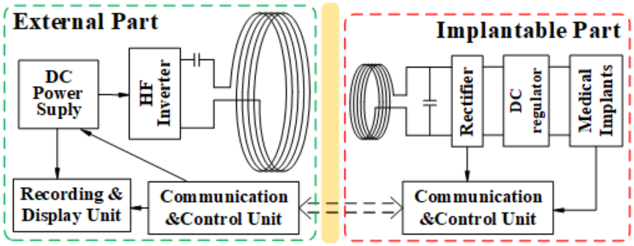

FIGURE 1. Wireless power transfer (WPT) system for IMDs.

inverter, which generates AC current in the transmitting coil. Then, the coupled AC voltage on the receiving coil is rectified and regulated to a DC voltage to supply the medical implants.

In practical IMD-WPT system, the variations of distance and alignment between two coils will result in the change of coupling condition. Furthermore, the equivalent load of IMDs will vary according to the operation mode or application. The variations of coupling and load may cause fluctuations in the output voltage of WPT system. To ensure the proper operation of IMDs, regulating output voltage of rectifier in response to variations of coupling and load are essential. A low dropout regulator or buck converter is commonly used to implement DC regulation [28], [29]. However, the DC regulator decreases the power efficiency of WPT system, and the size of DC regulator is an issue worth considering. In addition to the direct adjustment on the receiving side, the output voltage of WPT system is sensed and transferred to the transmitting side via data communication, then the DC power supply is adjusted accordingly to regulate the output voltage of WPT system [30], [31]. However, the extra communication module complicates receiving circuit and increases power consumption on the receiving side, which are not very suitable for the implantable WPT

If the output voltage of WPT system can be obtained based on the transmitting side information, adaptive adjustment of the input voltage can be implemented to regulate output voltage, which will eliminate the extra communication process to acquire output voltage. Much works of output voltage identification on transmitting side have been done in [32]–[36]. In [32], the energy injection mode and free resonant mode are used to detect load resistance before startup. However, it cannot track the variations of load afterwards. In [33] and [34], the load resistances are monitored by the information of transmitting side, but these approaches are all applied to the condition that mutual inductance is assumed to be known and constant. In [35] and [36], the method to monitor both mutual inductance and load resistance has been proposed for the WPT system with series-series (SS) topology. However, the operating frequency must not be the resonant frequency of the receiver circuit for accurate estimation [35]. And the system is operated at dual frequencies, one is for optimal power transfer and the other is for parameter estimation, which will increase the difficulty of system design [36].

In this paper, the output voltage identification for WPT system with series-parallel (SP) topology is presented in Section II. Section III presents a novel compensation network for WPT system, and describes the corresponding principle of output voltage identification. The characteristic analysis of the proposed topology is given in Section IV. Experimental results are provided in Section V. Finally, some conclusions are drawn in Section VI.

II. OUTPUT VOLTAGE IDENTIFICATION OF WPT SYSTEM WITH SP TOPOLOGY

The power demands of IMDs differ depending on application. For instance, the power consumption of capsule endoscopy and nerve stimulator usually ranges from 10 to 30mW [37]. However, the artificial heart consumes more power, like up to 15W [38]. For transmitting tens of milliwatts using WPT, the LC tank of the receiving coil is preferably tuned in parallel [39]. The equivalent circuit of the WPT system with SP topology is shown in Fig. 2, where L_1, L_2 and R_1, R_2 are the self-inductances and inherent resistances of the transmitting and receiving coils, respectively; C_1 and C_2 are the compensation capacitances of the transmitting and receiving sides, respectively. The mutual inductance between the transmitting and receiving coils is defined as M; the equivalent load is represented by the resistance R_L; u_s is the AC input voltage of the transmitting coil; i_1 is the input current; i_2 is the current along the receiving coil; u_o and i_o is the AC output voltage and current along the load R_L.

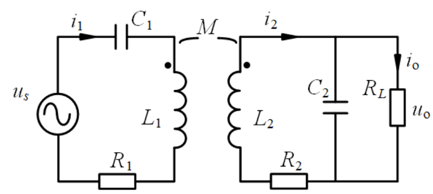

FIGURE 2. Equivalent circuit of the WPT system with SP topology.

According to Fig. 2, the KVL equation of the transmitting and receiving loops can be written as

$$\begin{bmatrix} \dot{u}_s \\ 0 \end{bmatrix} = \begin{bmatrix} R_1 + j\omega L_1 + \dfrac{1}{j\omega C_1} & -j\omega M \\ -j\omega M & R_2 + j\omega L_2 + \dfrac{R_L}{1 + j\omega R_L C_2} \end{bmatrix} \times \begin{bmatrix} \dot{i}_1 \\ \dot{i}_2 \end{bmatrix} \quad (1)$$

The industrial, scientific and medical (ISM) band frequency, such as 6.78 or 13.56 MHz, is commonly used as the resonant frequency of the WPT system. In this paper, the resonant frequency is chosen to be 6.78MHz. The resonant frequency is defined by

$$\omega = \frac{1}{\sqrt{L_1 C_1}} = \frac{1}{\sqrt{L_2 C_2}} \quad (2)$$

From (1), the output voltage of the WPT system can be derived as (3).

$$\dot{u}_o = \frac{-j\omega M R_L}{R_1(R_2 + j\omega L_2 + j\omega C_2 R_L R_2) + (\omega M)^2 (1 + j\omega C_2 R_L)} \cdot \dot{u}_s \quad (3)$$

Equation (3) indicates that the output voltage is a function of mutual inductance M and equivalent load R_L. As M and R_L are not constants but variables, we need to estimate M and R_L in order to identify U_o.

From (1), the input impedance can be expressed as

$$Z_{in} = R_1 + \frac{(\omega M)^2[R_2 + (\omega C_2)^2 R_L^2 R_2 + R_L]}{R_2^2 + (\omega C_2 R_L R_2 + \omega L_2)^2} - j\frac{\omega L_2(\omega M)^2}{R_2^2 + (\omega C_2 R_L R_2 + \omega L_2)^2} \quad (4)$$

and can be written as

$$Z_{in} = \frac{U_S}{I_1}\angle\theta = |Z_{in}|\cos\angle\theta + j|Z_{in}|\sin\angle\theta \quad (5)$$

where θ is the phase angle between u_s and i_1, U_S and I_1 are the amplitude of u_s and i_1, respectively.

When Z_{in} is obtained by measuring u_s and i_1, we have

$$|Z_{in}|\cos\angle\theta = R_1 + \frac{(\omega M)^2[R_2 + (\omega C_2)^2 R_L^2 R_2 + R_L]}{R_2^2 + (\omega C_2 R_L R_2 + \omega L_2)^2} \quad (6)$$

$$|Z_{in}|\sin\angle\theta = -\frac{\omega L_2(\omega M)^2}{R_2^2 + (\omega C_2 R_L R_2 + \omega L_2)^2} \quad (7)$$

Obviously, combining (6) and (7), the equation without M can be expressed as

$$\frac{|Z_{in}|\cos\angle\theta - R_1}{|Z_{in}|\sin\angle\theta} = -\frac{R_2 + R_L + (\omega C_2)^2 R_2 R_L^2}{\omega L_2} \quad (8)$$

Assumed that $A = \frac{|Z_{in}|\cos\angle\theta - R_1}{|Z_{in}|\sin\angle\theta}$, the estimated result of the equivalent load R_L can be obtained by solving the above equation. It is found that there are two solutions for R_L, the negative one should be ignored, and the reasonable solution is

$$R_{L,est} = \frac{-1 + \sqrt{1 - 4R_2(R_2 + A\omega L_2)(\omega C_2)^2}}{2R_2(\omega C_2)^2} \quad (9)$$

Then, on the basis of (7) and (9), the estimated mutual inductance M can be derived as

$$M_{est} = \frac{1}{\omega}\sqrt{\frac{|Z_{in}|\sin\angle\theta\left[R_2^2 + (\omega C_2 R_2 R_{L,est} + \omega L_2)^2\right]}{-\omega L_2}} \quad (10)$$

As shown in (9) and (10), the mutual inductance M and the equivalent load R_L can be estimated by measuring the input voltage and current of the WPT system (u_s and i_1), when the parameters of WPT system (L_1, L_2, R_1, R_2, C_1, C_2, ω) are constant and known. According to (1), the estimated amplitude of output voltage can be derived as

$$|U_o| = \frac{\omega M_{est} R_{L,est}}{\sqrt{R_2^2 + (\omega C_2 R_{L,est} R_2 + \omega L_2)^2}} I_1 \quad (11)$$

III. OUTPUT VOLTAGE IDENTIFICATION OF WPT SYSTEM WITH S-LCL TOPOLOGY

As seen from Section II, the load and mutual inductance can be estimated by the measured input information, then the estimated M and R_L are employed to identify U_o. Considering the measurement error, the output voltage identified by the estimated mutual inductance and load may easily deviate from the actual value. In [40], an LCL resonant network is inserted to the transmitting side of WPT system, in which the output voltage can keep constant despite the variations of load, an improved WPT system using LCL compensation network is proposed, in order to reduce the effect of the estimated errors on output voltage identification.

A. PRINCIPLE OF OUTPUT VOLTAGE IDENTIFICATION

The improved equivalent circuit of WPT system with S-LCL topology is presented in Fig. 3(a). The whole circuit can be divided into two parts. The power supply part is shown in Fig. 3(b), in which the AC voltage source is in series with filter inductor L_x, and the branch of AC source and L_x is in paralleled with filter capacitor C_x. The power transfer part is shown in Fig. 3(c), in which the transmitting coil is in series with capacitor C_1, the receiving coil is in paralleled with capacitor C_2 and the branch of inductor L_f and equivalent output load R_L; M is the mutual inductance between transmitting and receiving coils.

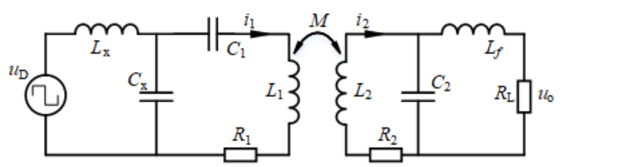

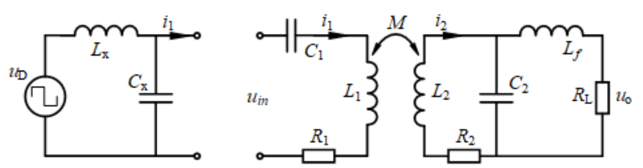

FIGURE 3. Improved WPT system with S-LCL topology. (a) Overall topology of WPT system; (b) Power supply part; (c) Power transfer part.

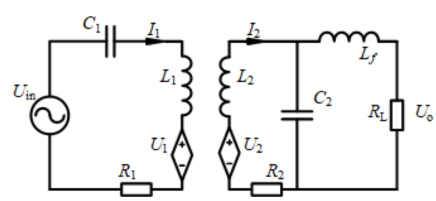

FIGURE 4. Equivalent circuit of power transfer part.

To analyze the power transfer process more clearly, the equivalent circuit of power transfer part in Fig. 3(c) is shown in Fig. 4. The operating frequency ω_0 of U_{in} is equal to resonant frequency, $U_1 = -j\omega_0 M I_2$ is the effective voltage induced in transmitting coil by I_2 through the mutual coupling M, and $U_2 = j\omega_0 M I_1$ is the effective voltage induced in the receiving coil by I_1 through the mutual coupling M.

To keep the system in resonance, the following equations should be satisfied,

$$\begin{cases} \omega_0 C_1 = \dfrac{1}{\omega_0 L_1} \\ \omega_0 C_2 = \dfrac{1}{\omega_0 L_2} + \dfrac{1}{\omega_0 L_f} \end{cases} \tag{12}$$

According to Fig. 4, because $\omega_0 L_2$ is much larger than R_2 in practice, the resistance of the receiving coil R_2 can be ignored, then the KVL equation of the receiving loop can be expressed as

$$U_2 = [\frac{U_o}{R_L}(R_L + j\omega_0 L_f)j\omega_0 C_2 + \frac{U_o}{R_L}]j\omega_0 L_2 + \frac{U_o}{R_L}(R_L + j\omega_0 L_f) \tag{13}$$

On the basis of (12), the output voltage can be derived by simplifying (13),

$$U_o = -\frac{L_f}{L_2}U_2 = -j\omega_0 M I_1 \frac{L_f}{L_2} \tag{14}$$

As shown in (14), the output voltage is irrelevant to the load, it is only related to the mutual inductance and the current on transmitting coil. According to KCL, the current along the receiving coil can be derived as

$$\begin{aligned} I_2 &= \frac{U_o}{R_L}(R_L + j\omega_0 L_f)j\omega_0 C_2 + \frac{U_o}{R_L} \\ &= \frac{U_o}{R_L}(j\frac{R_L}{\omega_0 L_2}\frac{\lambda+1}{\lambda} - \lambda) \end{aligned} \tag{15}$$

where $\lambda = L_f/L_2$.

According to Fig. 4, the KVL equation of the transmitting loop is

$$U_{in} = I_1 R_1 - j\omega_0 M I_2 \tag{16}$$

Combining (14) and (15), the input voltage of the transmitting loop can be expressed as

$$U_{in} = [R_1 + \lambda^2 \frac{\omega_0^2 M^2}{R_L} - j\frac{\omega_0 M^2(\lambda+1)}{L_2}]I_1 \tag{17}$$

Then, the corresponding input impedance Z_{in} can be obtained,

$$Z_{in} = R_1 + \lambda^2 \frac{\omega_0^2 M^2}{R_L} - j\frac{\omega_0 M^2(\lambda+1)}{L_2} \tag{18}$$

The unknown parameter in the imaginary part of Z_{in} is only M. Similar to the analysis in Section II, the imaginary part of input impedance can be acquired by measuring u_{in} and i_1. Consequently, the mutual inductance can be derived as

$$M_{est} = \sqrt{-\frac{L_2}{\omega_0(\lambda+1)}|Z_{in}|\sin\theta} \tag{19}$$

Substituting (19) into (14), the estimated output voltage is

$$|U_{o,est}| = \lambda I_1 \sqrt{-\frac{\omega_0 L_2}{(\lambda+1)}|Z_{in}|\sin\theta} \tag{20}$$

From (20), the estimated voltage can be obtained by measuring u_{in} and i_1, and the estimated result is independent of M and R_L.

According to (14), it should be noted that the output voltage is related to I_1, which means the regulation of output voltage can be accomplished by controlling the current along transmitting coil. To simplify the control, the power supply shown in Fig. 3(b) is used.

Normally, u_D is a square wave with constant magnitude. If the resonant frequency of LC filter equals to the operating frequency of u_D, that is

$$\omega_0 = \frac{1}{\sqrt{L_X C_X}} \tag{21}$$

Then the relationship between the magnitude of input voltage U_D and the magnitude of input current I_1 can be expressed as

$$I_1 = -j\sqrt{\frac{C_X}{L_X}}U_D \tag{22}$$

As shown in (22), the input current I_1 can be adjusted by regulating U_D.

B. ERROR ANALYSIS OF ESTIMATED OUTPUT VOLTAGE

In practice, the existence of R_2 may make the estimated result deviate from the actual value. To verify the feasibility of (20), the inherent resistance R_2 of the receiving coil is taken into consideration in this part. According to the receiving loop in Fig. 4, the KVL equation is rewritten as

$$U_2 = [\frac{U_o}{R_L}(R_L + j\omega_0 L_f)j\omega_0 C_2 + \frac{U_o}{R_L}](j\omega_0 L_2 + R_2) + \frac{U_o}{R_L}(R_L + j\omega_0 L_f) \tag{23}$$

As $U_2 = j\omega M I_1$, the output voltage can be derived by simplifying (23),

$$U_o = \frac{j\omega_0 M I_1}{(j\frac{\lambda+1}{\lambda}\frac{R_2}{\omega_0 L_2} - \lambda\frac{R_2}{R_L} - \frac{1}{\lambda})} = \frac{j\omega_0 M I_1}{-b + ja} \tag{24}$$

where $a = \frac{\lambda+1}{\lambda}\frac{R_2}{\omega_0 L_2}$, $b = \lambda\frac{R_2}{R_L} + \frac{1}{\lambda}$.

Then, combining (15) and (24), the input voltage U_{in} can be expressed as

$$U_{in} = I_1 R_1 + I_1(\omega_0 M)^2 \frac{\frac{a^2}{R_2} + \frac{\lambda b}{R_L} - j\frac{a}{\lambda R_2}}{a^2 + b^2} \tag{25}$$

According to (25), the imaginary part of input impedance can be expressed as

$$|Z_{in}|\sin\theta = -\frac{a(\omega_0 M)^2}{\lambda R_2(a^2 + b^2)} \tag{26}$$

Thus, the actual mutual inductance can be obtained by

$$M_{real} = \frac{1}{\omega_0}\sqrt{-\frac{\lambda R_2(a^2+b^2)\,|Z_{in}|\sin\theta}{a}} \tag{27}$$

Substituting (27) into (24), the actual output voltage can be derived as

$$\left|U_{o,real}\right| = \lambda I_1\sqrt{-\frac{\omega_0 L_2}{\lambda+1}\,|Z_{in}|\sin\theta} \tag{28}$$

Then, on the basis of (20) and (28), the ratio of estimated output voltage and actual output voltage can be obtained as

$$\kappa = \left|\frac{U_{o.est}}{U_{o.real}}\right| = 1 \tag{29}$$

Obviously, equation (29) proves the feasibility of the output voltage estimated method.

IV. CHARACTERISTICS OF WPT SYSTEM WITH S-LCL TOPOLOGY

According to (24), it can be noted that the existence of R_2 causes the output voltage to be related to the load. To analyze the effect of load variation on the output voltage, the actual output voltage U_o versus load R_L under different L_f is shown in Fig.5, where M is assumed to be a constant value 0.1μH. It is found that the output voltage rises quickly with the increase of load at the range of 0 to 500Ω, and has slight increase when R_L is larger than 500Ω. As L_f increases, the output voltage increases faster at the range of 500 to 2500Ω.

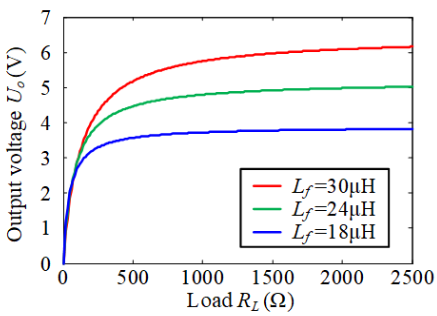

FIGURE 5. Actual output voltage U_o versus R_L.

Fig. 5 indicates that the output voltage with S-LCL topology does not have load-independence in practice. However, on the basis of (29), it can conclude that the estimated voltage is the same as the actual one, which means even if the load changes affect the output voltage, the proposed estimation method or (20) is correct.

The power transfer efficiency η of the WPT system with S-LCL topology can be expressed as

$$\eta_{S-LCL} = \frac{\frac{U_o^2}{R_L}}{I_1^2R_1 + I_2^2R_2 + \frac{U_o^2}{R_L}} \tag{30}$$

Then, combining (15), (24) and (30), the power transfer efficiency can be derived as

$$\begin{aligned}\eta_{S-LCL} &= \frac{(\omega_0 M)^2L_2^2L_f^2}{L_2^4R_1R_L + M^2(L_2+L_f)^2R_2R_L + (\omega_0M)^2L_2^2L_f^2} \\ &= \frac{(\omega_0M)^2}{\frac{R_1R_L}{\lambda^2} + M^2(\frac{1+\lambda}{\lambda L_2})^2R_2R_L + (\omega_0M)^2}\end{aligned} \tag{31}$$

As shown in (31), the transfer efficiency η is related to not only the parameters of coils and load, but also λ. Then the optimal λ should be determined by considering its effect on the transfer efficiency of the WPT system. Assuming ω_0 = 6.78MHz, L_1 = 4.4 μH, R_1 = 1.1Ω, L_2 = 1.22μH, R_2 = 0.2Ω, M = 0.08μH, the transfer efficiency η versus λ under different R_L is shown in Fig.6, where the load R_L is selected to 500Ω, 1500Ω and 2500Ω, respectively. It is noted that as λ increases, η increases. Besides, η decreases with the increase of the load. The transfer efficiency η versus λ under different mutual inductance M is shown in Fig.7, where M is selected to 0.06μH, 0.08μH and 0.1μH, respectively. Similarly, η increases when λ or M increases.

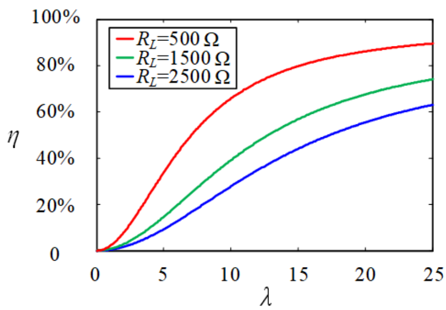

FIGURE 6. Transfer efficiency η versus λ under different R_L, where M = 0.08μH.

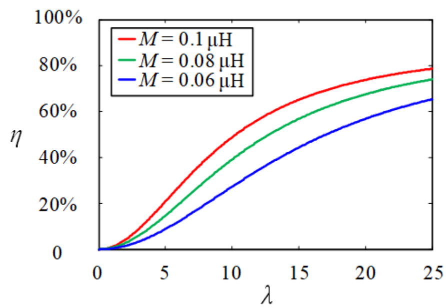

FIGURE 7. Transfer efficiency η versus λ under different M, where R_L=1500Ω.

According to Fig. 6 and Fig. 7, λ should be as large as possible to ensure relatively high transfer efficiency. Since the equivalent load resistance of milliwatt-level IMDs is approximately in the range of 500Ω to 2500Ω [7], [39], and the mutual inductance of our prototype is approximately 0.05μH to 0.1μH, the transfer efficiency η versus load R_L and mutual inductance M is shown in Fig. 8 when λ = 20. It is found that the transfer efficiency can reach a higher value when load and mutual inductance vary.

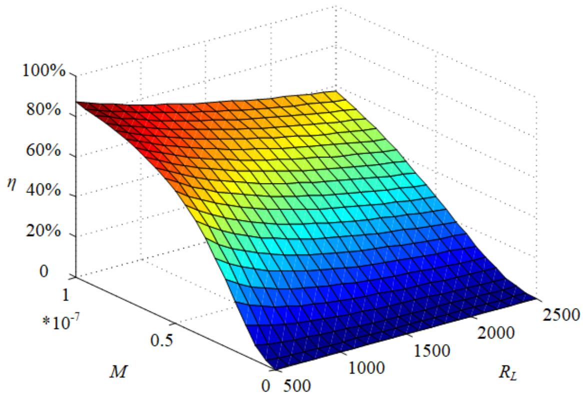

FIGURE 8. Transfer efficiency η versus RL and M, where λ=20.

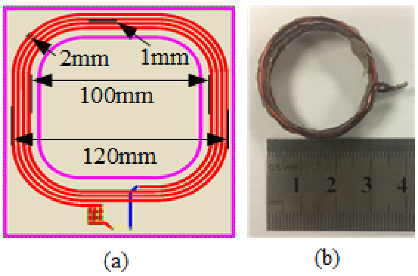

FIGURE 9. Configuration of coils. (a) Transmitting coil, (b) Receiving coil.

V. EXPERIMENTAL RESULTS

High-frequency class-D amplifier is commonly used in WPT system for low power applications. In this paper, a class-D amplifier with fixed frequency ($\omega_0 = 6.78$MHz) is selected. Power MOSFET SUD06N10 is selected as the power switch, and the corresponding driver IC is SI8271.

The transmitting and receiving coils of the prototype are shown in Fig. 9. The shape of the transmitting coil is rounded square with a number of turns of 4, an inner side length of 100 mm, an outer side length of 120 mm, a copper wire width of 2 mm, a pitch of 1 mm and a wire thickness of 0.035 mm. The receiving coil has a diameter of 30 mm and a height of 10 mm, a wire diameter of 1 mm, and a number of turns of 6.

The experimental set-up of the WPT prototype with S-LCL topology is shown in Fig. 10. The prototype parameters are measured by Impedance Analyzer WK6500B and summarized in Table 1. According to the analysis in Section III, the inductance L_f should be large to ensure a high efficiency. Considering λ is about 20, the inductance L_f is 24.83μH. The DC input voltage of class-D amplifier u_{dc} is 5V, the distance between two coils is 5cm, the equivalent load resistance is 1200Ω. Experimental waveforms are shown in Fig.11, where u_o is the output voltage of the load on receiving side, u_D and i_1 are the output voltage of the class D amplifier and the current on transmitting coil, respectively.

To verify the output voltage estimation method, the input voltage u_{in} and input current i_1 are captured by a Tektronix DPO4034 Digital Oscilloscope. Then the sampled data of u_{in} and i_1 are processed in MATLAB, and the fundamental amplitude and phase angle of u_{in} and i_1 are obtained. According to previous analysis in Section III, the amplitude of the output voltage can be calculated. Then the estimated amplitude of output voltage and actual output voltage are shown in Fig. 12, where the DC voltage represents for the estimated amplitude of output voltage. In Fig. 12(a), the coil distance is 3cm, the amplitude of actual output voltage is about 4.2V, and the estimated result is in accord with the actual value. Similarly, in Fig. 12 (b) and (c), despite the output voltage changes with distance, the DC voltage is still at the peak

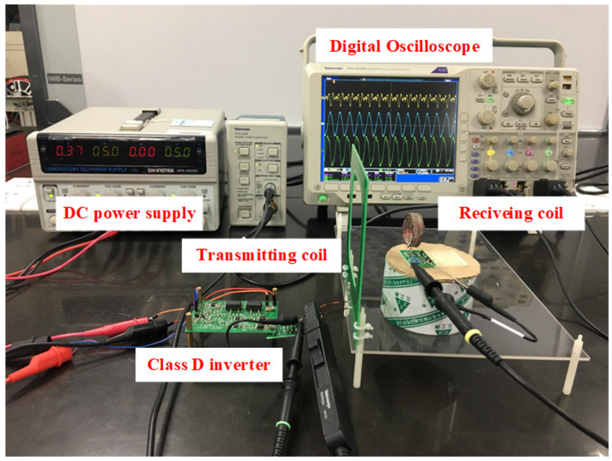

FIGURE 10. Experimental set-up.

TABLE 1. Prototype parameters.

Symbol	Value
L_1	4.4μH
R_1	1.1Ω
L_2	1.22μH
R_2	0.2Ω
C_1	123.32 pF
C_2	464.26 pF
L_f	24.83μH
L_X	1.02μH
C_X	539.58 pF

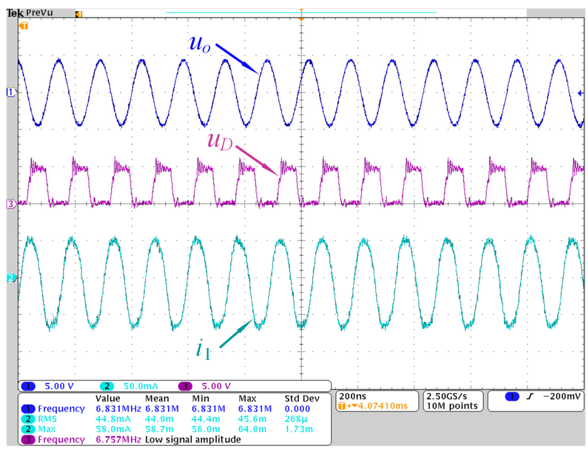

FIGURE 11. Experimental waveforms.

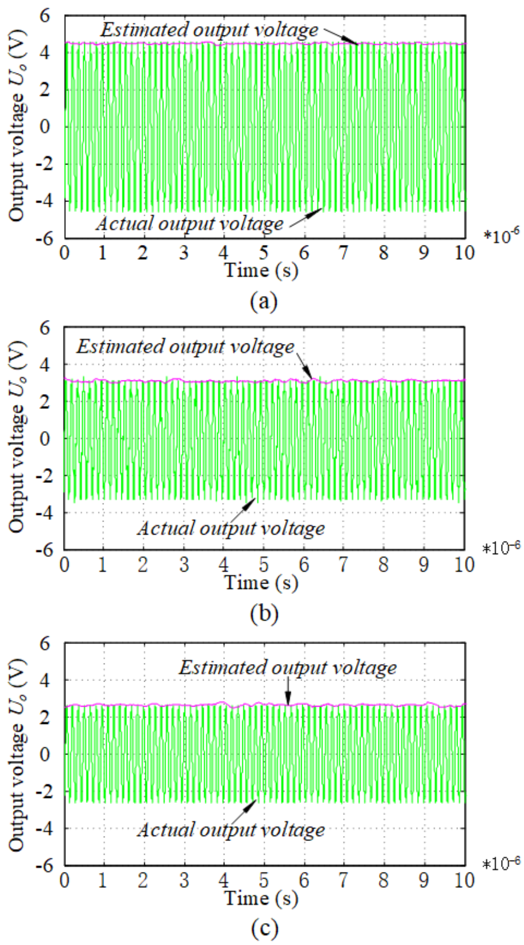

FIGURE 12. Actual output voltage and estimated output voltage. (a) Coils distance is 3cm. (b) Coils distance is 5cm. (c) Coils distance is 6cm.

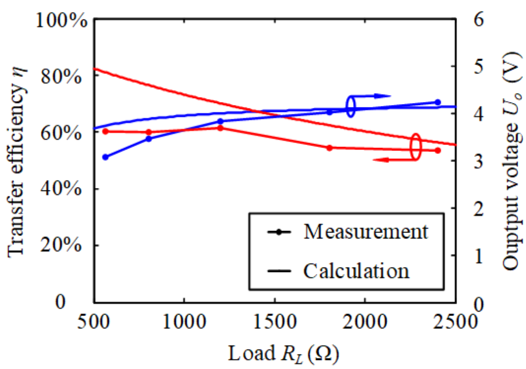

FIGURE 13. Measured and calculated transfer efficiency and amplitude of output voltage at different loads.

of the AC voltage, which indicates the estimated results are accurate.

The amplitude of load voltage and transfer efficiency with different load can be calculated based on (19) and (31). Fig. 13 shows the measured and calculated transfer efficiency and amplitude of load voltage when the distance between two coils is fixed at 5cm and the load resistance R_L changes from 560 to 2400Ω. From Fig. 13, the measured transfer

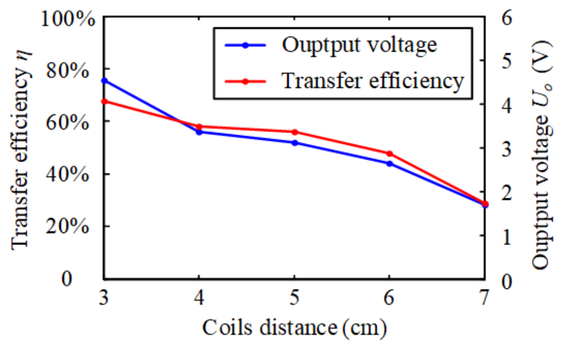

FIGURE 14. Measured transfer efficiency and amplitude of output voltage at different coil distances.

efficiency and the output voltage have the same trend as the calculated results. At the resonance frequency 6.78MHz, the ESR of inductor L_f is about tens of ohms, and L_f is in series with load resistance. When the load resistance drops, the current on load increases accordingly. As a result, the voltage drop and power consumption on the ESR of inductance L_f increase. Therefore, when the load resistance decreases, the measurement result is lower than the theoretical value.

The transfer efficiency and amplitude of load voltage at different coils distance are presented in Fig. 14, in which the load resistance is 1200Ω. As the distance between two coils increases, the mutual inductance reduces. Correspondingly, the transfer efficiency and output voltage decrease.

VI. CONCLUSIONS

This paper presents a method to identify the output voltage for implantable WPT system, in which only the input voltage and current along the receiving coil are needed to be measured. Furthermore, an improved WPT system with S-LCL compensation network has been proposed, where the output voltage identification is not related to the load and mutual inductance, and the output voltage estimation is simple and accurate. Experimental set-ups have been used for practical evaluation. The experimental results verified the feasibility of output voltage identification based on transmitting side information, and the estimated output voltage based on the measured voltage and current on transmitting side is consistent with the measured output voltage, which demonstrates the validity of proposed output voltage identification for WPT system with S-LCL compensation network. It is concluded that the identified voltage can be used to regulate output voltage for free-positioning implantable WPT system. In addition, the experimental results show that the transfer efficiency is over 50% when the distance between transmitting and receiving coils is within 6cm, which provides an important guidance for implantable WPT applications.

REFERENCES

[1] B. B. Lee, "Method and apparatus for monitoring heart function in a subcutaneously implanted device," U.S. Patent 7 035 684, Apr. 25, 2006.
[2] D. Vilkomerson and T. Chilipka, "Implantable Doppler system for self-monitoring vascular grafts," in *Proc. IEEE Ultrason. Symp.*, Montreal, QC, Canada, Aug. 2004, pp. 461–465.

[3] F. P. Bozider and B. Breyer, "Ultrasound methods and implantable medical devices using same," U.S. Patent 7 037 266, May 2, 2006.
[4] J. Chen, X. Cheng, P. Lin, and S. Zhou, "Implantable ultrasound emitter array for medical applications," in *Proc. 19th IEEE Int. Conf. Micro Electro Mech. Syst.*, Istanbul, Turkey, Jan. 2006, pp. 422–425.
[5] S. C. Tang, T. L. T. Lun, Z. Guo, K.-W. Kwok, and N. J. McDannold, "Intermediate range wireless power transfer with segmented coil transmitters for implantable heart pumps," *IEEE Trans. Power Electron.*, vol. 32, no. 5, pp. 3844–3857, May 2017, doi: 10.1109/TPEL.2016.2584558.
[6] F.-G. Zeng, "Trends in cochlear implants," *Trends Amplification*, vol. 8, no. 1, pp. 1–34, 2004.
[7] K. Agarwal, R. Jegadeesan, Y.-X. Guo, and N. V. Thakor, "Wireless power transfer strategies for implantable bioelectronics: methodological review," *IEEE Rev. Biomed. Eng.*, vol. 10, pp. 136–161, Mar. 2017, doi: 10.1109/RBME.2017.2683520.
[8] R. Puers, R. Carta, and J. Thoné, "Wireless power and data transmission strategies for next-generation capsule endoscopes," *J. Micromech. Microeng.*, vol. 21, no. 5, p. 054008, Apr. 2011, doi: 10.1088/0960-1317/21/5/054008.
[9] W. Xin, G. Yan, and W. Wang, "Study of a wireless power transmission system for an active capsule endoscope," *Int. J. Med. Robot. Comput. Assist. Surg.*, vol. 6, no. 1, pp. 113–122, 2010.
[10] M. R. Basar, M. Y. Ahmadm, J. Cho, and F. Ibrahim, "Stable and high-efficiency wireless power transfer system for robotic capsule using a modified helmholtz coil," *IEEE Trans. Ind. Electron.*, vol. 64, no. 2, pp. 1113–1122, Feb. 2017, doi: 10.1109/TIE.2016.2614268.
[11] S. Kim, J. S. Ho, L. Y. Chen, and A. S. Y. Poon, "Wireless power transfer to a cardiac implant," *Appl. Phys. Lett.*, vol. 101, no. 7, p. 073701, 2012, doi: 10.1063/1.4745600.
[12] M. A. Karami and D. J. Inman, "Powering pacemakers from heartbeat vibrations using linear and nonlinear energy harvesters," *Appl. Phys. Lett.*, vol. 100, no. 4, p. 042901, 2012.
[13] G. B. Joun and B. H. Cho, "An energy transmission system for an artificial heart using leakage inductance compensation of transcutaneous transformer," *IEEE Trans. Power Electron.*, vol. 13, no. 6, pp. 1013–1022, Nov. 1998, doi: 10.1109/63.728328.
[14] R. Puers and G. Vandevoorde, "Recent progress on transcutaneous energy transfer for total artificial heart systems," *Artif. Organs*, vol. 25, no. 5, pp. 400–405, 2001, doi: 10.1046/j.1525-1594.2001.025005400.x.
[15] M. R. Carhart, J. He, R. Herman, S. D'Luzansky, and W. T. Willis, "Epidural spinal-cord stimulation facilitates recovery of functional walking following incomplete spinal-cord injury," *IEEE Trans. Neural Syst. Rehabil. Eng.*, vol. 12, no. 1, pp. 32–42, Mar. 2004, doi: 10.1109/TNSRE.2003.822763.
[16] H. Huang, J. He, R. Herman, and M. R. Carhart, "Modulation effects of epidural spinal cord stimulation on muscle activities during walking," *IEEE Trans. Neural Syst. Rehabil. Eng.*, vol. 14, no. 1, pp. 14–23, Mar. 2006, doi: 10.1109/TNSRE.2005.862694.
[17] C.-H. Hsu, S.-B. Tseng, Y.-J. Hsieh, and C.-C. Wang, "One-time-implantable spinal cord stimulation system prototype," *IEEE Trans. Biomed. Circuits Syst.*, vol. 5, no. 5, pp. 490–498, Oct. 2011, doi: 10.1109/TBCAS.2011.2157152.
[18] S. Kunnumpurath, R. Srinivasagopalan, and N. Vadivelu, "Spinal cord stimulation: Principles of past, present and future practice: A review," *J. Clin. Monitor. Comput.*, vol. 23, no. 5, pp. 333–339, 2009, doi: 10.1007/s10877-009-9201-0.
[19] Q. Xu, D. Hu, B. Duan, and J. He, "A fully implantable stimulator with wireless power and data transmission for experimental investigation of epidural spinal cord stimulation," *IEEE Trans. Neural Syst. Rehabil. Eng.*, vol. 23, no. 4, pp. 683–692, Jul. 2015, doi: 10.1109/TNSRE.2015.2396574.
[20] F. Zhang, X. Liu, S. A. Hackworth, R. J. Sclabassi, and M. Sun, "Wireless energy delivery and data communication for biomedical sensors and implantable devices," in *Proc. IEEE 35th Annu. Northeast Bioeng. Conf.*, Boston, MA, USA, Apr. 2009, pp. 1–2.
[21] R. Das and H. Yoo, "A multiband antenna associating wireless monitoring and nonleaky wireless power transfer system for biomedical implants," *IEEE Trans. Microw. Theory Techn.*, vol. 65, no. 7, pp. 2485–2495, Jul. 2017, doi: 10.1109/TMTT.2017.2647945.
[22] P. Houghton, "Living with the Jarvik 2000: A five-plus year experience," *Artif. Organs*, vol. 30, no. 5, pp. 322–323, May 2006, doi: 10.1111/j.1525-1594.2006.00221.x.
[23] D. S. Bennett and D. Brookoff, "Complex regional pain syndromes (reflex sympathetic dystrophy and causalgia) and spinal cord stimulation," *Pain Med.*, vol. 7, no. s1, pp. S64–S96, May 2006, doi: 10.1111/j.1526-4637.2006.00124.x.
[24] A. Kim, M. Ochoa, R. Rahimi, and B. Ziaie, "New and emerging energy sources for implantable wireless microdevices," *IEEE Access*, vol. 3, pp. 89–98, 2015, doi: 10.1109/ACCESS.2015.2406292.
[25] M. W. Baker and R. Sarpeshkar, "Feedback analysis and design of RF power links for low-power bionic systems," *IEEE Trans. Biomed. Circuits Syst.*, vol. 1, no. 1, pp. 28–38, Mar. 2007, doi: 10.1109/TBCAS.2007.893180.
[26] A. K. Ram Rakhyani, S. Mirabbasi, and M. Chiao, "Design and optimization of resonance-based efficient wireless power delivery systems for biomedical implants," *IEEE Trans. Biomed. Circuits Syst.*, vol. 5, no. 1, pp. 48–63, Feb. 2011, doi: 10.1109/TBCAS.2010.2072782.
[27] X. Li, C.-Y. Tsui, and W.-H. Ki, "A 13.56 MHz wireless power transfer system with reconfigurable resonant regulating rectifier and wireless power control for implantable medical devices," *IEEE J. Solid-State Circuits*, vol. 50, no. 4, pp. 978–989, Apr. 2015, doi: 10.1109/JSSC.2014.2387832.
[28] K.-G. Moh *et al.*, "A fully integrated 6W wireless power receiver operating at 6.78 MHz with magnetic resonance coupling," in *IEEE Int. Solid-State Circuits Conf. (ISSCC) Dig. Tech. Papers*, Feb. 2013, pp. 1–3.
[29] J.-H. Choi, S.-K. Yeo, S. Park, J.-S. Lee, and G.-H. Cho, "Resonant regulating rectifiers (3R) operating for 6.78 MHz resonant wireless power transfer (RWPT)," *IEEE J. Solid-State Circuits*, vol. 48, no. 12, pp. 2989–3001, Dec. 2013, doi: 10.1109/JSSC.2013.2287592.
[30] R. R. Harrison *et al.*, "A low-power integrated circuit for a wireless 100-electrode neural recording system," *IEEE J. Solid-State Circuits*, vol. 42, no. 1, pp. 123–133, Jan. 2007, doi: 10.1109/JSSC.2006.886567.
[31] S. Mandal and R. Sarpeshkar, "Power-efficient impedance-modulation wireless data links for biomedical implants," *IEEE Trans. Biomed. Circuits Syst.*, vol. 2, no. 4, pp. 301–315, Dec. 2008, doi: 10.1109/TBCAS.2008.2005295.
[32] Z. H. Wang, Y. P. Li, Y. Sun, C. S. Tang, and X. Lv, "Load detection model of voltage-fed inductive power transfer system," *IEEE Trans. Power Electron.*, vol. 28, no. 11, pp. 5233–5243, Nov. 2013, doi: 10.1109/TPEL.2013.2243756.
[33] S. Nutwong, A. Sangswang, S. Naetiladdanon, and E. Mujjalinvimut, "Load monitoring and output voltage control for SP topology IPT system using a single-side controller without any output measurement," in *Proc. 18th Eur. Conf. Power Electron. Appl.*, Karlsruhe, Germany, Sep. 2016, pp. 1–10.
[34] J. Yin, D. Lin, C.-K. Lee, and S. Y. R. Hui, "A systematic approach for load monitoring and power control in wireless power transfer systems without any direct output measurement," *IEEE Trans. Power Electron.*, vol. 30, no. 3, pp. 1657–1667, Mar. 2015, doi: 10.1109/TPEL.2014.2317183.
[35] J. Yin, D. Lin, T. Parisini, and S. Y. R. Hui, "Front-end monitoring of the mutual inductance and load resistance in a series–series compensated wireless power transfer system," *IEEE Trans. Power Electron.*, vol. 31, no. 10, pp. 7339–7352, Oct. 2016, doi: 10.1109/TPEL.2015.2509962.
[36] E. Chung, J. Lee, and J.-I. Ha, "System conditions monitoring method for a wireless cellular phone charger," in *Proc. Int. Power Electron. Appl. Conf. Expo.*, Shanghai, China, Nov. 2014, pp. 639–643.
[37] T. Sun, X. Xie, G. Li, Y. Gu, Y. Deng, and Z. Wang, "A two-hop wireless power transfer system with an efficiency-enhanced power receiver for motion-free capsule endoscopy inspection," *IEEE Trans. Biomed. Eng.*, vol. 59, no. 11, pp. 3247–3254, Nov. 2012, doi: 10.1109/TBME.2012.2206809.
[38] P. Si, A. P. Hu, S. Malpas, and D. Budgett, "A frequency control method for regulating wireless power to implantable devices," *IEEE Trans. Biomed. Circuits Syst.*, vol. 2, no. 1, pp. 22–29, Mar. 2008, doi: 10.1109/TBCAS.2008.918284.
[39] R. Jegadeesan, S. Nag, K. Agarwal, N. V. Thakor, and Y.-X. Guo, "Enabling wireless powering and telemetry for peripheral nerve implants," *IEEE J. Biomed. Health Informat.*, vol. 19, no. 3, pp. 958–970, May 2015, doi: 10.1109/JBHI.2015.2424985.
[40] Y. Wang, Y. Yao, X. Liu, D. Xu, and L. Cai, "An LC/S compensation topology and coil design technique for wireless power transfer," *IEEE Trans. Power Electron.*, vol. 33, no. 3, pp. 2007–2025, Mar. 2018, doi: 10.1109/TPEL.2017.2698002.

XIANGTIAN MENG was born in Anhui, China, in 1992. He received the B.S. degree in electrical engineering and automation from the Shanghai University of Electric Power, Shanghai, China, in 2014. He is currently pursuing the M.S. degree in power electronics and power drives with the South China University of Technology, Guangzhou, China.

His main research direction is wireless power transfer system for implanted medical devices.

DONGYUAN QIU was born in Guangdong, China, in 1972. She received the B.Sc. and M.Sc. degrees from the South China University of Technology, Guangzhou, China, in 1994 and 1997, respectively, and the Ph.D. degree from the City University of Hong Kong, Hong Kong, in 2002.

She is currently a Professor with the School of Electric Power, South China University of Technology. She has authored or co-authored two books and over 100 papers, and holds 80 patents. Her main research interests include wireless power transfer, fault diagnosis, and sneak circuit analysis of power electronic systems. She is an Associate Editor of the IEEE Transactions on Power Electronics.

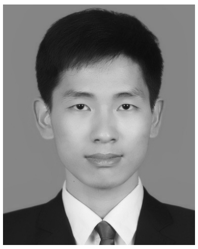

MANHAO LIN was born in Guangdong, China, in 1995. He received the B.S. degree in electrical engineering and automation from the South China University of Technology, Guangzhou, China, in 2018, where he is currently pursuing the M.S. degree in power electronics and power drives.

His current research interest is wireless power transfer technology.

SAI CHUN TANG was born in Hong Kong, in 1972. He received the B.Eng. degree (Hons.) and the Ph.D. degree in electronic engineering from the City University of Hong Kong, Hong Kong, in 1997 and 2000, respectively. He was a Research Fellow with the City University of Hong Kong after he graduated. In 2001, he joined the National University of Ireland, Galway, as a Visiting Academic, and then the Laboratory for Electromagnetic and Electronic Systems, Massachusetts Institute of Technology, Cambridge, MA, USA, in 2002.

Since 2004, he has been with the Radiology Department, Brigham, and the Women's Hospital, Harvard Medical School, Boston, MA, USA, for the development of ultrasound diagnosis devices and noninvasive treatment systems using high-intensity focused ultrasound. Since 2008, he has been a Faculty in Radiology with the Harvard Medical School. His current research interests include wireless power transfer, electronic medical devices, high-frequency electromagnetism, low-profile power converter design, and analog electronics.

BO ZHANG was born in Shanghai, China, in 1962. He received the B.Sc. degree in electrical engineering from Zhejiang University, Hangzhou, China, in 1982, the M.Sc. degree in power electronics from Southwest Jiaotong University, Chengdu, China, in 1988, and the Ph.D. degree in power electronics from the Nanjing University of Aeronautics and Astronautics, Nanjing, China, in 1994.

He is currently a Professor with the School of Electric Power, South China University of Technology, Guangzhou, China. He has authored or co-authored five books and over 400 technical papers, and he holds over 100 patents. His current research interests include nonlinear analysis, modeling and control of power electronic converters, and wireless power transfer applications.